Biologically Inspired Nano-Manufacturing

PIs:

- **Anthony Muscat, Chemical and Environmental Engineering, UA**
- **Megan McEvoy, Biochemistry and Molecular Biophysics, BIO5 Institute, UA**
- **Masud Mansuripur, College of Optical Sciences, UA**

Graduate Students:

- **Amber Young, PhD candidate, College of Optical Sciences, UA**
- **Sam Jayakanthan, PhD candidate, Biochemistry and Molecular Biophysics, UA**
- **Shawn Miller, PhD candidate, College of Optical Sciences, UA**
- **Rahul Jain, PhD candidate, Chemical and Environmental Engineering, UA**

Undergraduate Student:

- **Ben Mills, Chemical and Environmental Engineering, UA**

Other Researchers:

- **Zhengtao Deng, Postdoctoral Fellow, ChEE & Optical Sciences, UA**
- **Gary Fleming, Postdoctoral Fellow, Chemical and Environmental Engineering, UA**

Objectives

- **Minimize costs of materials, energy, and water to fabricate nanoscale devices using bio-based strategy**
- **Exploit homogeneity, mild reaction conditions, and specificity of active biological molecules**
- **Grow 3D structures to achieve scalable architecture**
- **Employ additive, bottom up patterning methods**

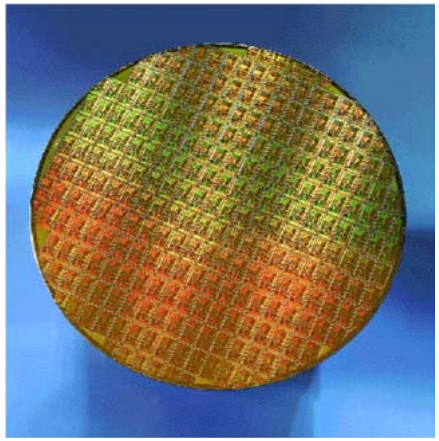

Semiconductor fabs consume

- **Water equivalent to 30,000-50,000 residents**
- **Energy equivalent to 10,800 single family homes**
  - 130 million kWh/yr

Water, energy, and materials costs escalate

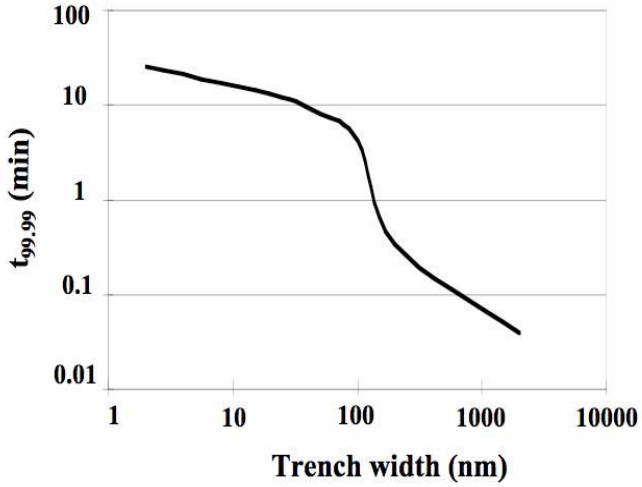

Subtractive vs. Additive Processing

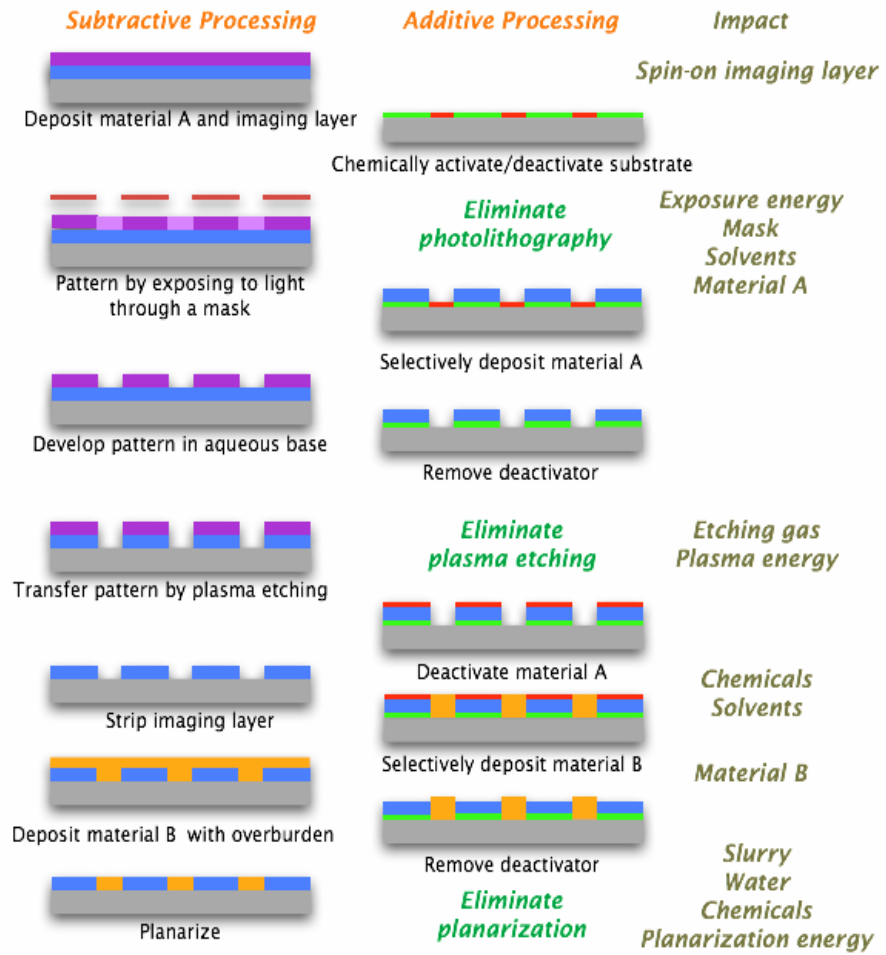

Biological materials hold potential for sustainable manufacturing

many biological materials are stable and active at near neutral pH and moderate temperature

small scale (sub 10nm) is achievable

consistent sizes of biological materials may be relatively easy to reproduce

Biological materials in nano-manufacturing

biological molecules as templates or scaffolds

virus particles as scaffolds to assemble inorganic material into wires

S. R. Whaley, D. S. English, E. L. Hu, P. F. Barbara and A. M. Belcher, "*Selection of peptides with semiconductor binding specificity for directed nanocrystal assembly*" Nature 405 (2000) 665-668

P. J. Yoo, K. T. Nam, J. Qi, S.-K. Lee, J. Park, A. M. Belcher, P. T. Hammond, "*Spontaneous assembly of viruses on multilayered polymer surfaces*," Nat. Mater. 5 (2006) 234-40.

A. Fortig, R. Jordan, K. Graf, G. Schiavon, O. Purrucker, M. Tanaka, "*Solid-supported biomimetic membranes with tailored lipopolymer tethers*," Macromol. Sym. 210 (2004) 329-338.

R. Naumann, S. M. Schiller, F. Giess, B. Grohe, K. B. Hartman, I. Karcher, I. Koper, J. Lubben, K. Vasilev, W. Knoll, "*Tethered lipid Bilayers on ultraflat gold surfaces*," Langmuir 19 (13) (2003) 5435-5443.

biological materials as pores

electrical current measurements through ion channels incorporated into membranes

M. Andersson, H. M. Keizer, C. Zhu, D. Fine, A. Dodabalapur, R. S. Duran, "*Detection of Single Ion Channel Activity on a Chip Using Tethered Bilayer Membranes*," Langmuir 23 (6) (2007) 2924-2927

Process Goal: Utilize Metal Transport Proteins to Deposit Array of Metal Dots

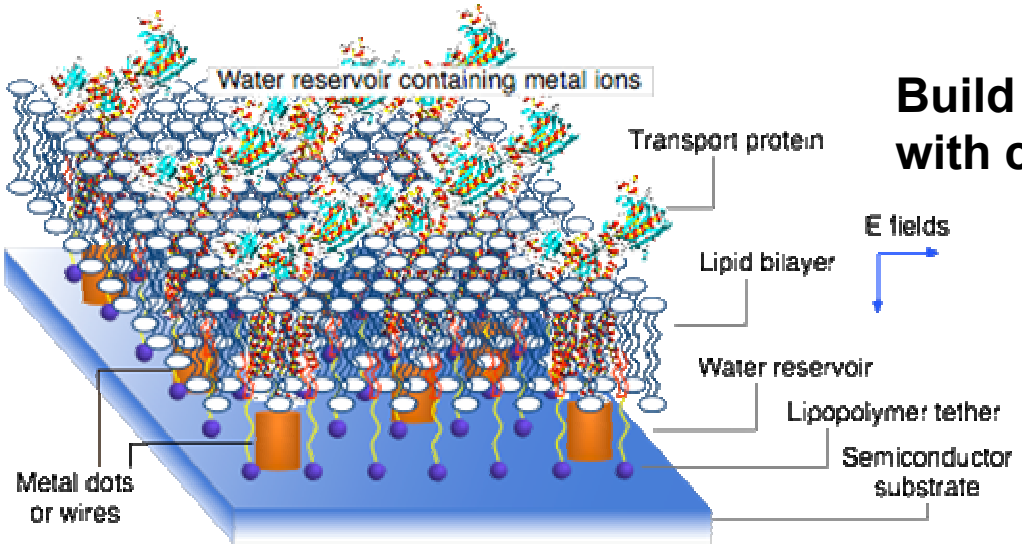

Mild fabrication conditions

Build structures not possible with current technology

Process Goal: Deposit Array of Metal Dots

Biochemistry of metal transport proteins
Megan McEvoy/UA

Characterize bio & inorganic structures using scanning probe and optical techniques
Masud Mansuripur/UA

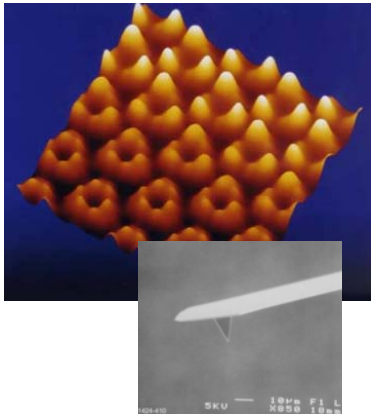

Selective deposition
Glen Wilk, Eric Shero, Christophe Pomarede Steve Marcus/ASM

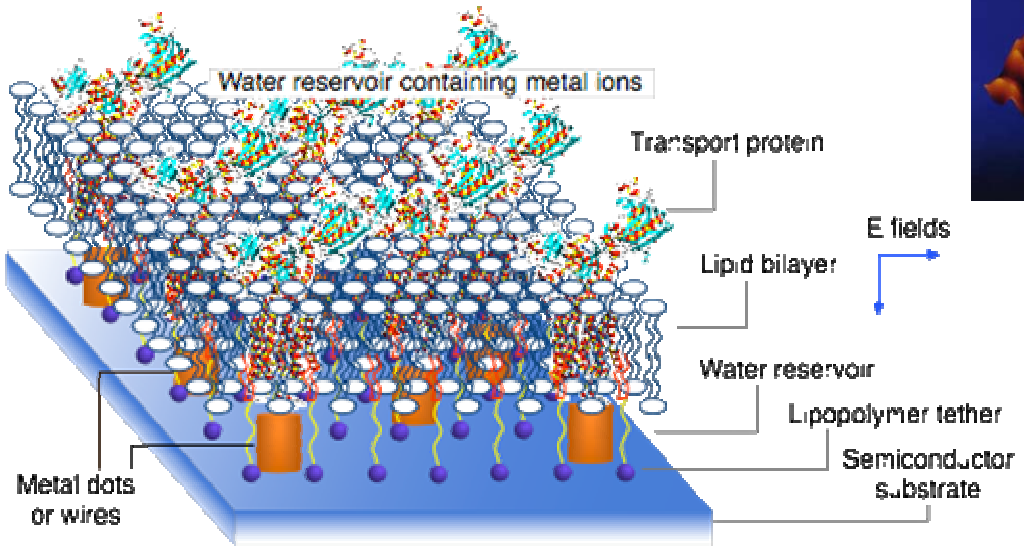

Pattern surfaces and build structures
Anthony Muscat/UA

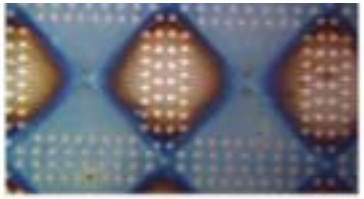

Semiconductor surface preparation
Harald Okorn-Schmidt, Zach Hatcher, Jeremy Klitzke/SEZ

ESH Metrics and Impact

Sustainability metrics			
Process	Water l/bit/masking layer	Energy J/bit/masking layer	Materials g/bit/masking layer
Subtractive 32 nm*	3.3×10^{-10}	1.5×10^{-12} EUV	2.9×10^{-16}
Additive	3.6×10^{-13}	9.2×10^{-17}	1.8×10^{-19}

The amount of WEM resources per bit per masking layer was calculated using the estimates included in the 32 nm technology node of the 2005 ITRS roadmap30 for the conventional approach using extreme ultraviolet (EUV) photolithography and on a detailed process flow for the bioinspired approach. The energy required to build an array of metal dots is estimated from the ATP used by the transport protein. Let one square cylindrical dot (3 nm diameter, 3 nm high) hold one bit of information and the entire array of dots define a masking layer based on subtractive patterning terminology. Let each Cu^{2+} ion transported consume one ATP molecule and the free energy of hydrolysis of ATP is ≈ -31 kJ/mole. The energy required to grow a 21 nm^3 dot by biological self-assembly is 9.2×10^{-17} J/bit/masking layer. The water and materials (metal) requirements were calculated using a material balance. Materials includes only the metal required and does not include photoresist and chemicals in the subtractive approach and the transport proteins or lipid bilayer in the additive approach.

*D. Herr, Extending Charge-based Technology to its Ultimate Limits: Selected Research Challenges for Novel Materials and Assembly Methods. Presentation at the NSF/SRC EBSM Engineering Research Center Review Meeting: February 24, 2006.

Metal transport proteins

- Metal transport proteins naturally occur in many organisms as resistance systems to allow the organism's survival in metal contaminated environments.

- Transport proteins are known for many metals and semiconductors, since high concentrations of these atoms are toxic to most cells.

  S. Silver, L. T. Phung, "*A bacterial view of the periodic table: genes and proteins for toxic inorganic ions*," J. Ind. Microbio. Biotech. 32 (11-12) (2005) 587-605

- Natural selection or protein engineering holds promise to create transport systems for other metals where natural transporters are not currently known.

Bacterial cation transport systems

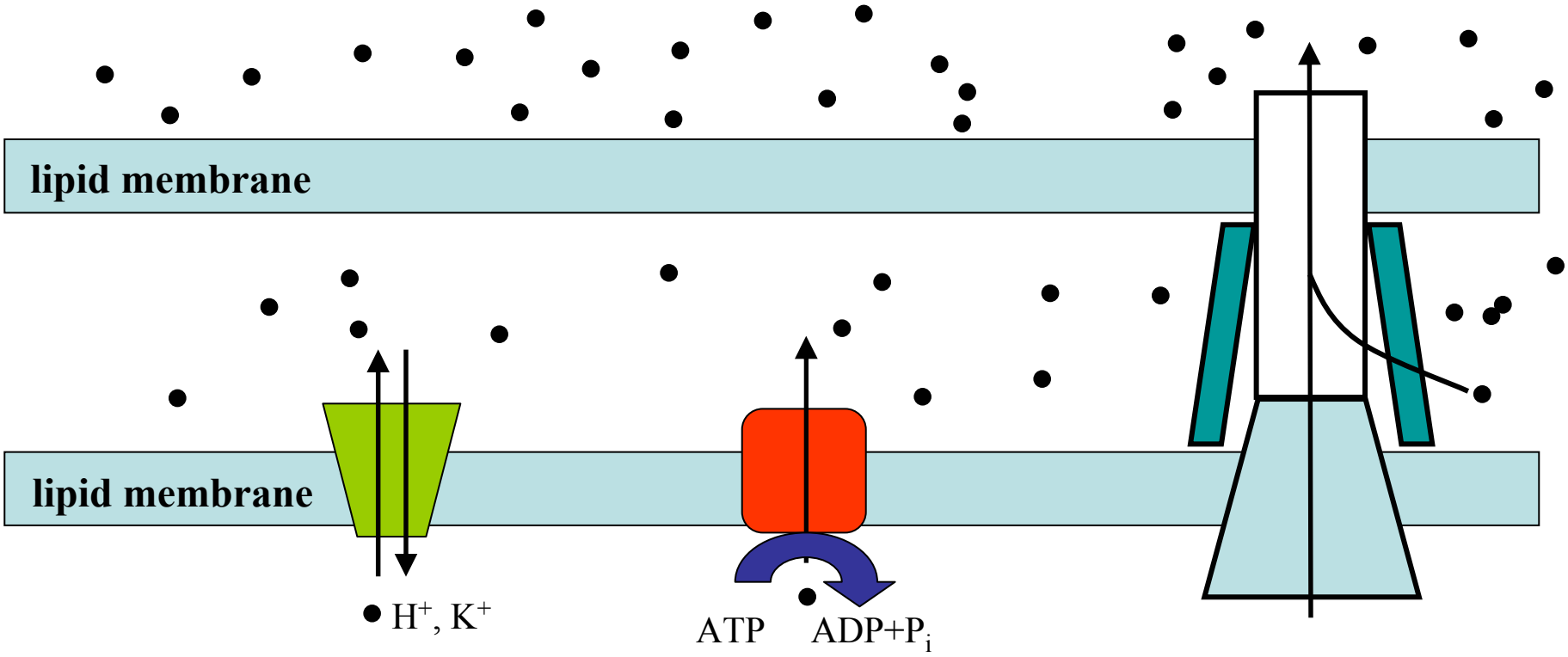

chemiosmotic transporters
Zn^{2+}, Co^{2+}, Cd^{2+},
Ni^{2+}, Cu^{2+}, Ag^+, Fe^{2+}

ATP-driven transporters
H^+, K^+, Na^+, Mg^{2+}, Ca^{2+}, Cu^{2+}
Cu^+, Ag^+, Cd^{2+}, Zn^{2+}, Pb^{2+}

RND transporters
Cu^+, Ag^+, Cd^{2+}, Co^{2+},
Zn^{2+}, Ni^{2+}

Methods and Approach

Metal Transport Protein: CopB from *Archaeoglobus fulgidus*

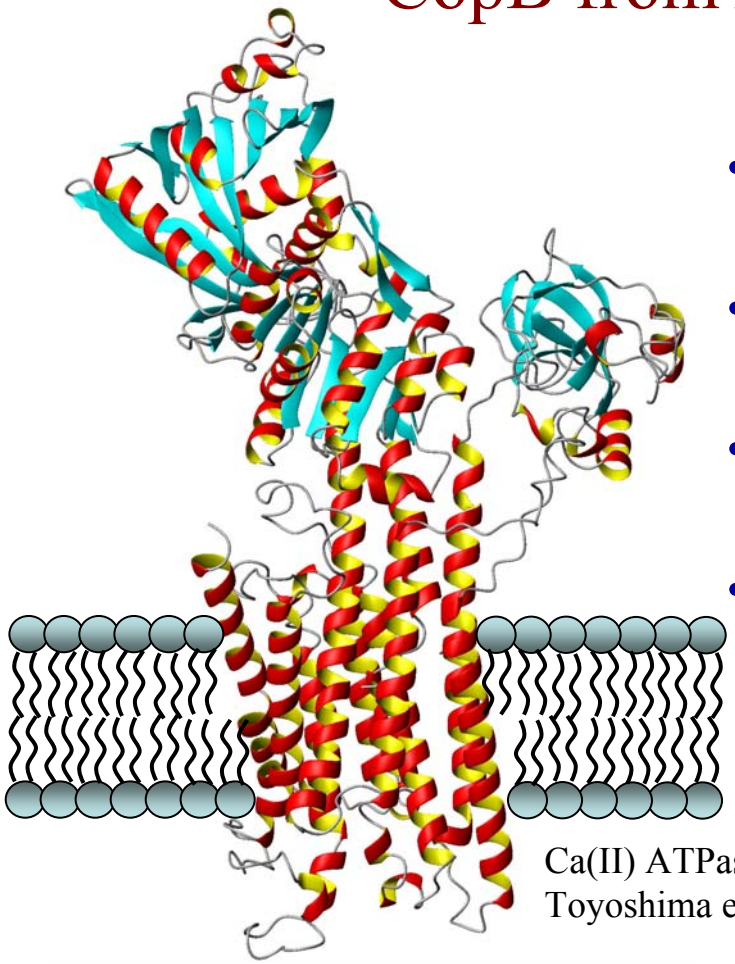

Ca(II) ATPase
Toyoshima et al (2000) Nature 405, 647-655

- Cu(II) transport activity in artificial membranes
- Energy source: Adenosine triphosphate (ATP)
- Enhanced stability at room temperature
- Recombinant protein purified from *E. coli*

The approximate dimensions of the Cu(II) transporter CopB

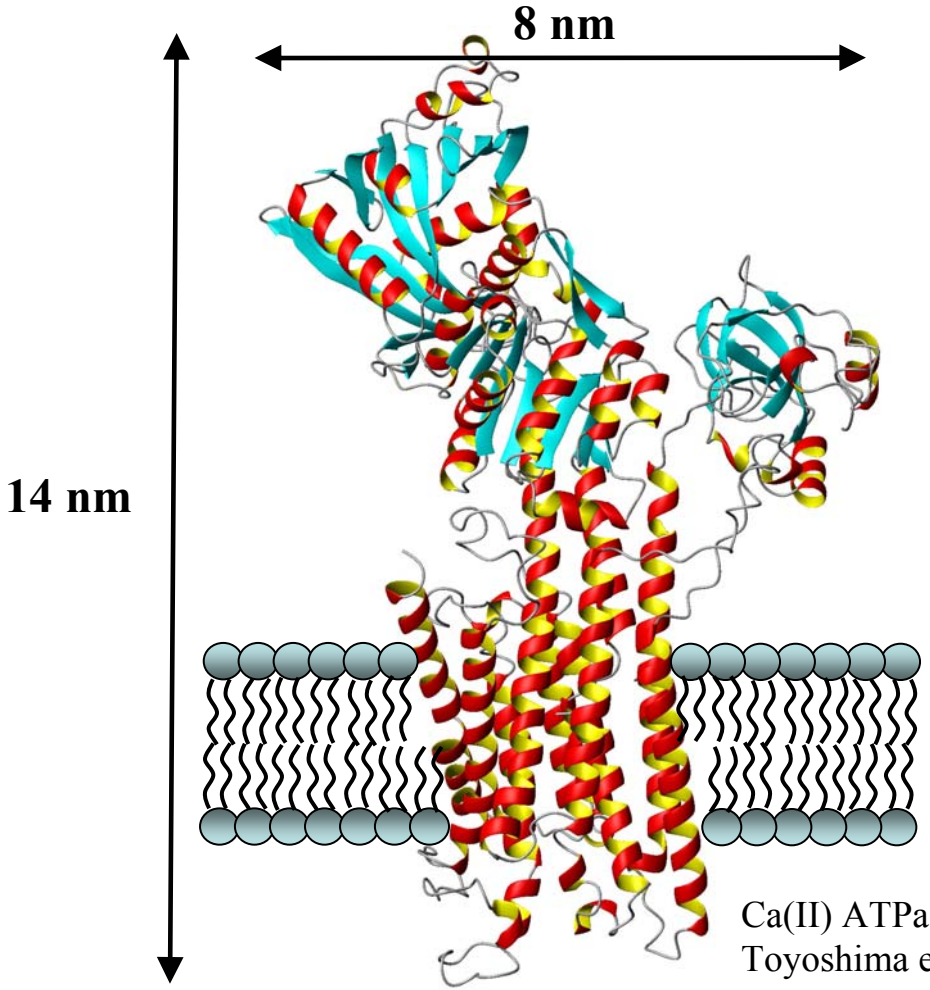

Ca(II) ATPase
Toyoshima et al (2000) Nature 405, 647-655

Activation of CopB by metals

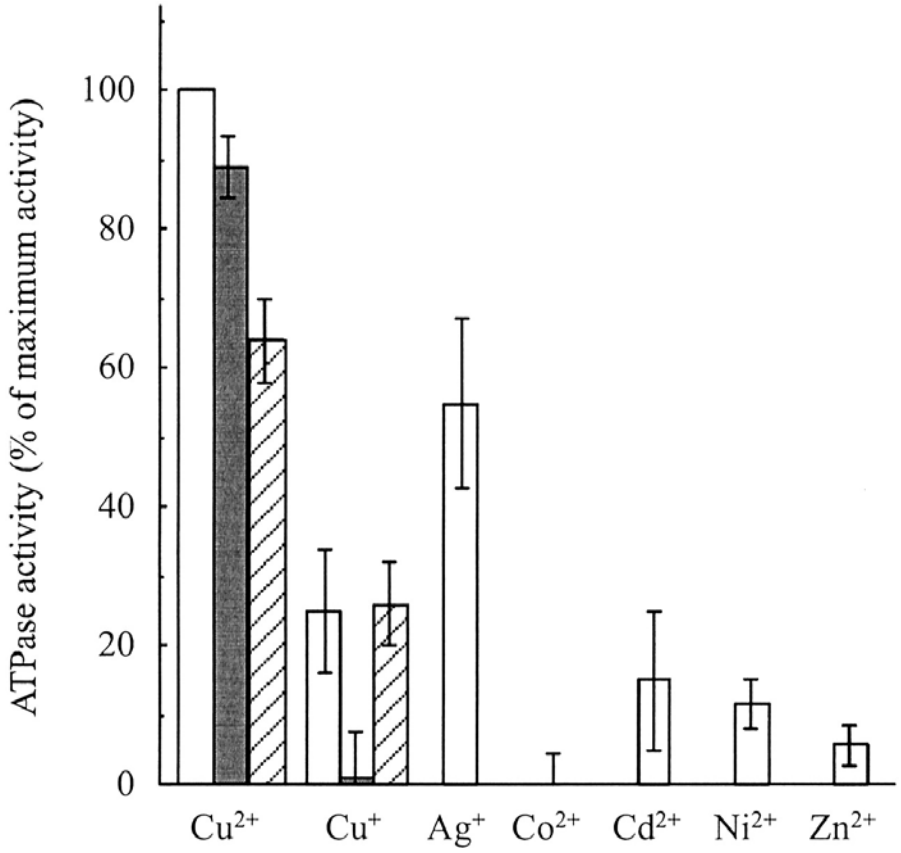

Activation of CopB-ATPase by metals. Final concentration of each tested metal ion was 1 µM, which is a saturating concentration for all of them. 2.5 mM DTT was included in Cu+-containing assay mixture. *Bars* indicate activity in the presence of each metal (*white*) upon the addition of BCA (*gray*) or 20 mM cysteine (*striped*). 100% = 5.0 µmol/mg/h.

Mana-Capelli, S. et al. J. Biol. Chem. 2003;278:40534-40541

Preparation of CopB

copB gene

isolation of the gene encoding CopB from *Archaeoglobus fulgidus*

E. coli expression plasmid

insertion of the *copB* DNA into an *E. coli* expression plasmid

CopB protein expression in *E. coli*

DNA containing *copB* is introduced into *E. coli* followed by growth of *E. coli* with induction of overexpression of CopB

Affinity chromatography to isolate CopB protein

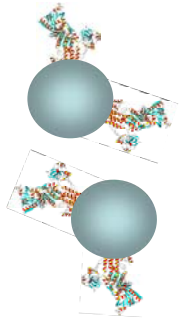

Purified CopB in vesicles

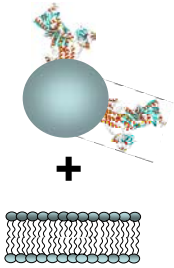

Fusion of vesicles and lipid bilayer

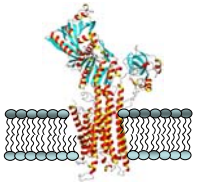

CopB incorporated in lipid bilayer

Visualization of proteins to monitor the purification process

Polyacrylamide gel electrophoresis to separate proteins of different molecular weight. Proteins are stained with a dye (coomassie blue) for detection.

The quantity and purity of the protein can be determined with this method.

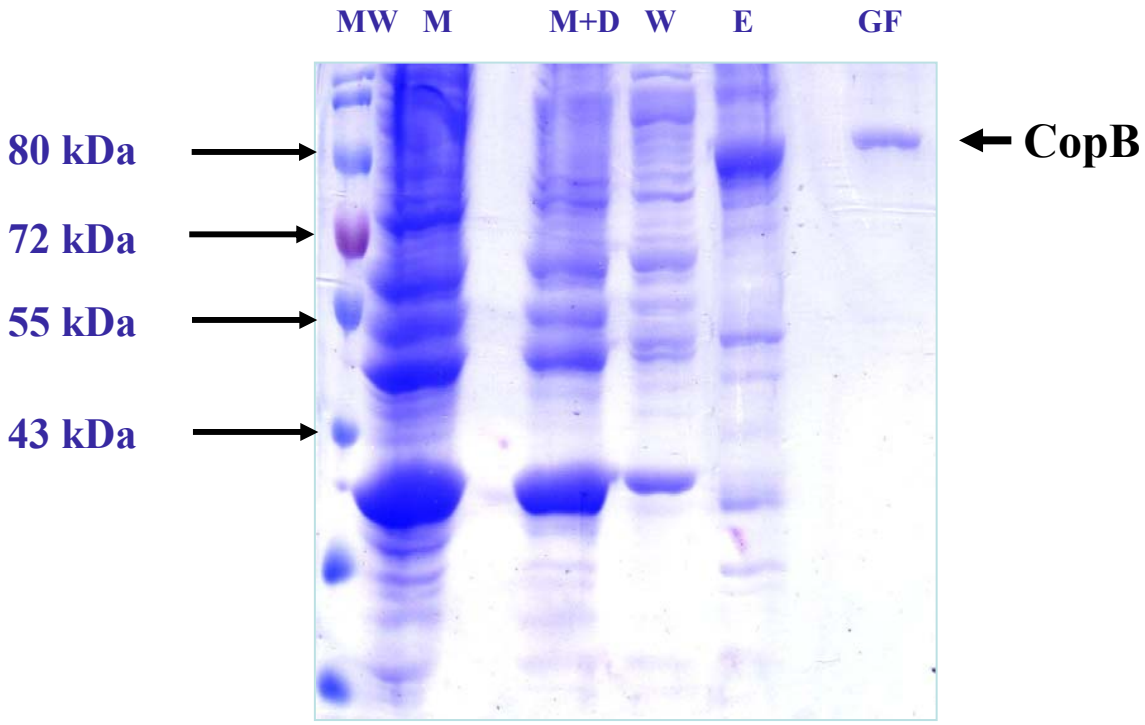

10% SDS-PAGE gel of affinity purified CopB Lanes: M- total membrane protein, M-D – detergent solubilized protein, W – wash with 30 mM imidazole, E – elution with 400 mM imidazole, GF – sample purified using size exclusion (Sephacryl S-300)

Purified CopB shows ATPase activity

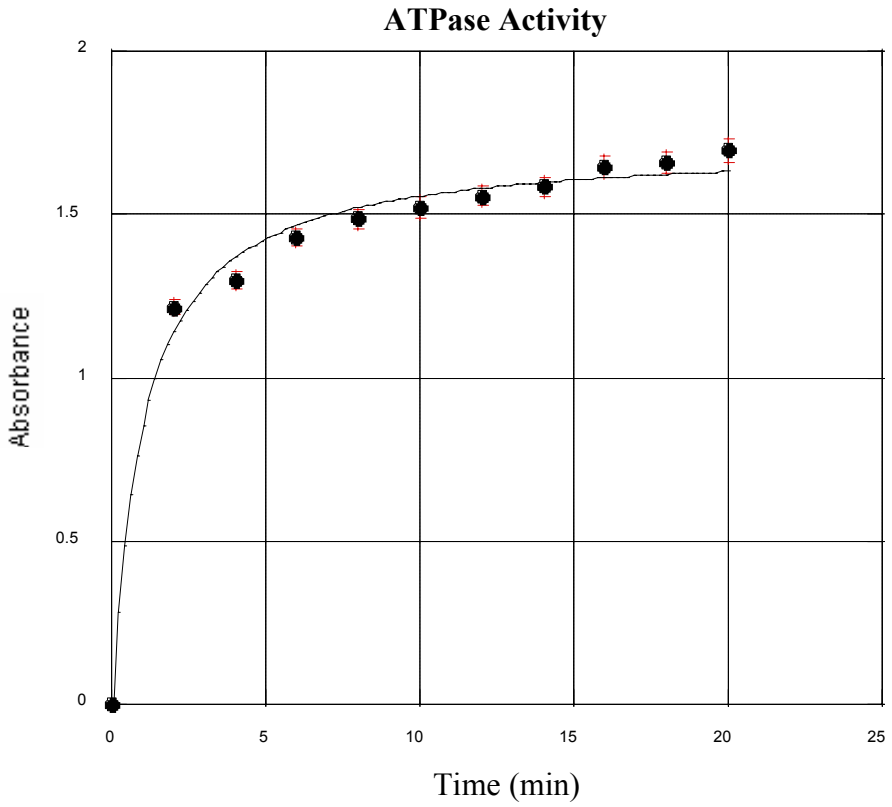

The activity of the purified protein was tested using a standard ATPase activity assay (Lanzetta *et al*., (1979) *Anal. Biochem.* 100, 95-97) at
The ATPase assay mixture contained 50 mM Tris-Cl, pH 5.7, 3 mM $MgCl_2$, 3 mM ATP, 400 mM NaCl and membranes at a concentration of 0.7 mg/ml. The detergent/phospholipid (DDM/Asolectin) mixture was maintained at 0.1%. 50 mM Cysteine and 1 mM $CuSO_4$ were added to the mixture.

Next step: Insertion of CopB into lipid bilayer and demonstration of transport and deposition

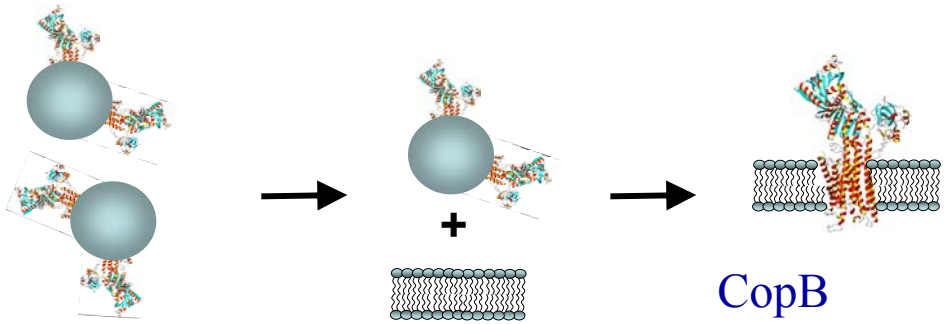

purified protein in detergent has activity

Lipid Bilayer Characterization

Lipid Bilayer

- **Verify lipid bilayer using patchclamp, AFM, impedance measurements and ellipsometry**
- **Examine large coverage area**
- **Investigate surface uniformity**

Lipid Bilayer Formation

Continuous Lipid Bilayer

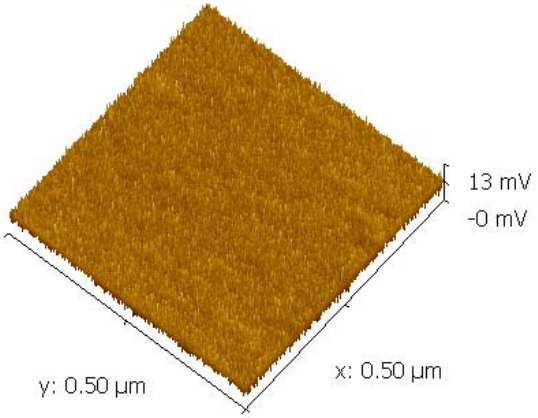

Discontinuous Lipid Bilayer

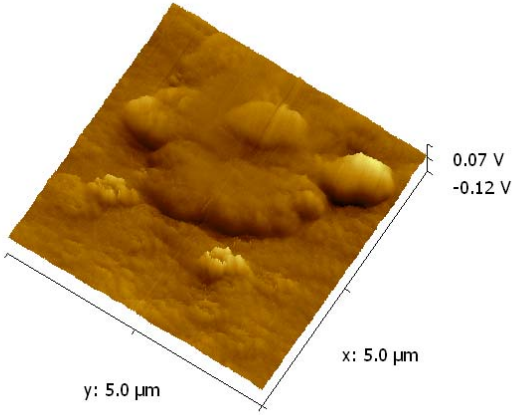

- Formation of bilayer occurs spontaneously
- Bilayer thickness is 3-4 nm
- AFM images depict piecewise uniformity

Bilayer Deposition

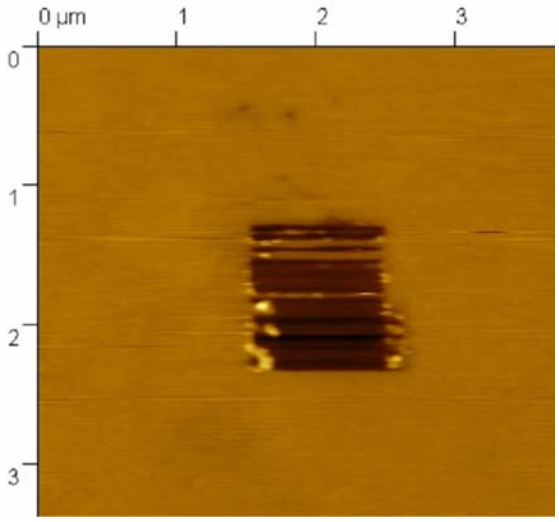

1 µm square hole dug in lipid membrane. Observe smooth bilayer surface. Note excess material piled at edge of hole.

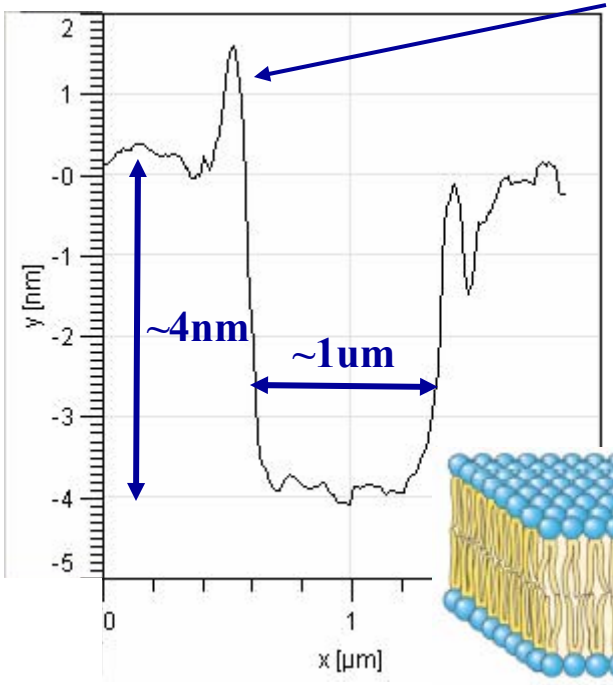

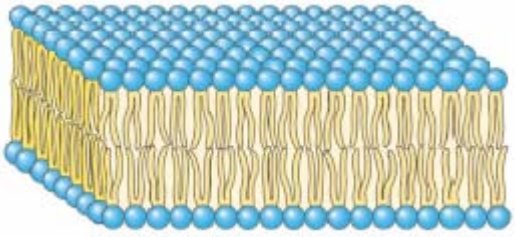

Material piled at edge of hole by AFM tip

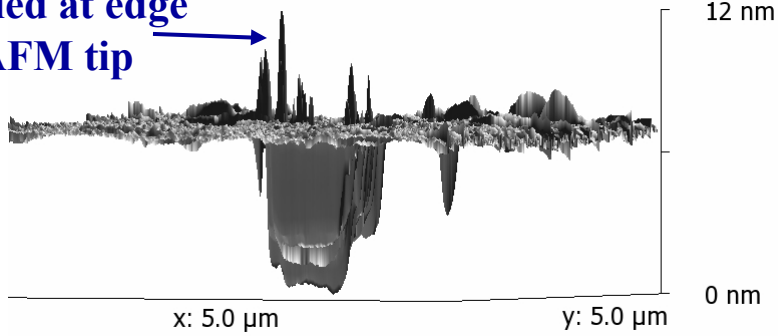

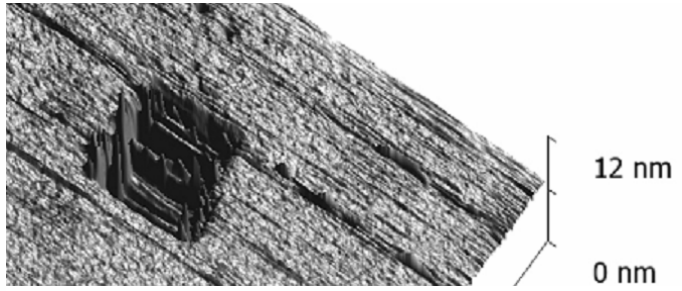

3D representations of hole dug in bilayer.

Surface Patterning

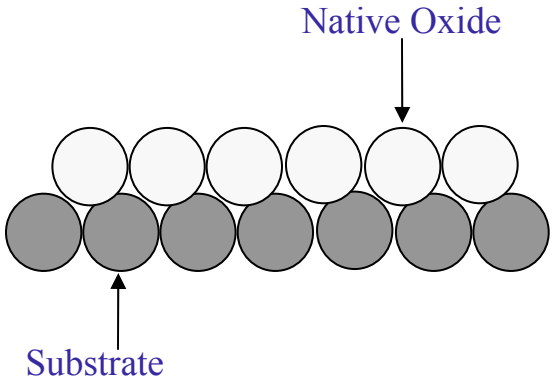

(i) Surface Preparation

Cleaning performed by chemical etching

Characterized by X-ray Photoelectron Spectroscopy, Atomic Force Microscopy, and Temperature Programmed Desorption Spectroscopy

Possible substrates for use:
Si, Ge, GaAs, InAs, InP, InSb

Surface Patterning

(ii) Surface Functionalization

Surface chemistry used to modify surface to introduce patterning and to attach tether molecules

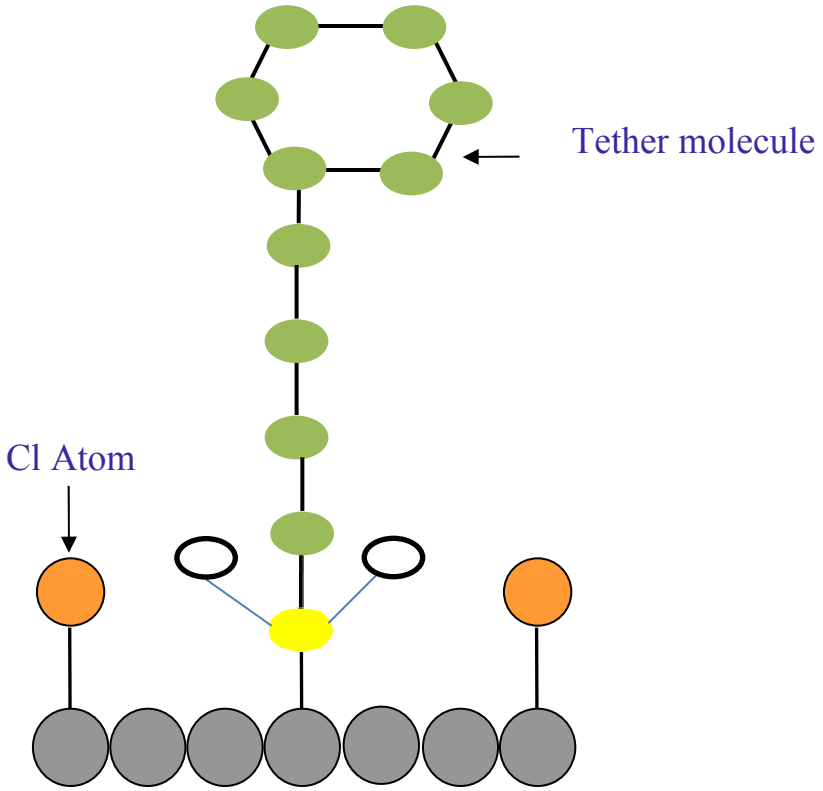

Patterning Step: UV/Cl_2, NH_3

Tethers = Amines (benzylbutylamine, dibutylamine, ethylamine), Benzene, Pyridine

Surface Patterning

(iii) Lipid Bilayer Addition

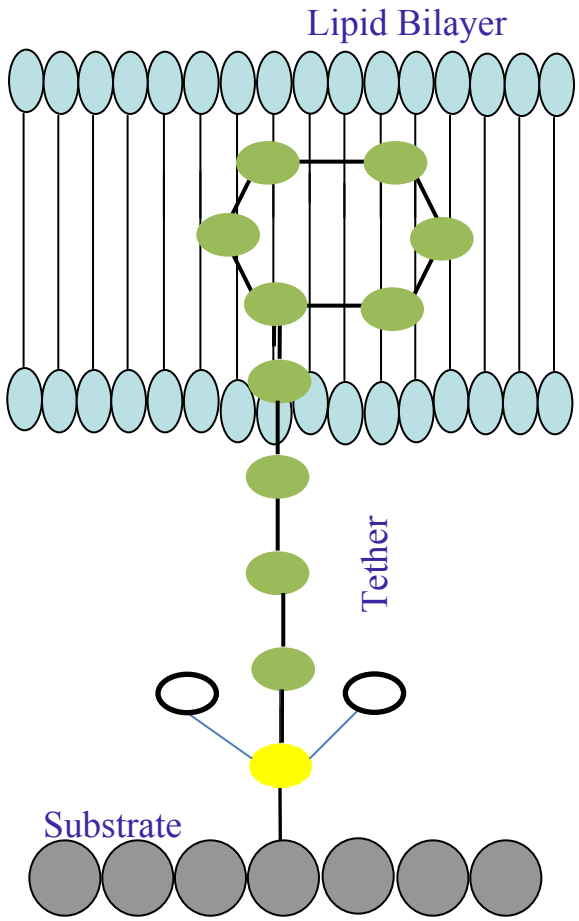

Integration

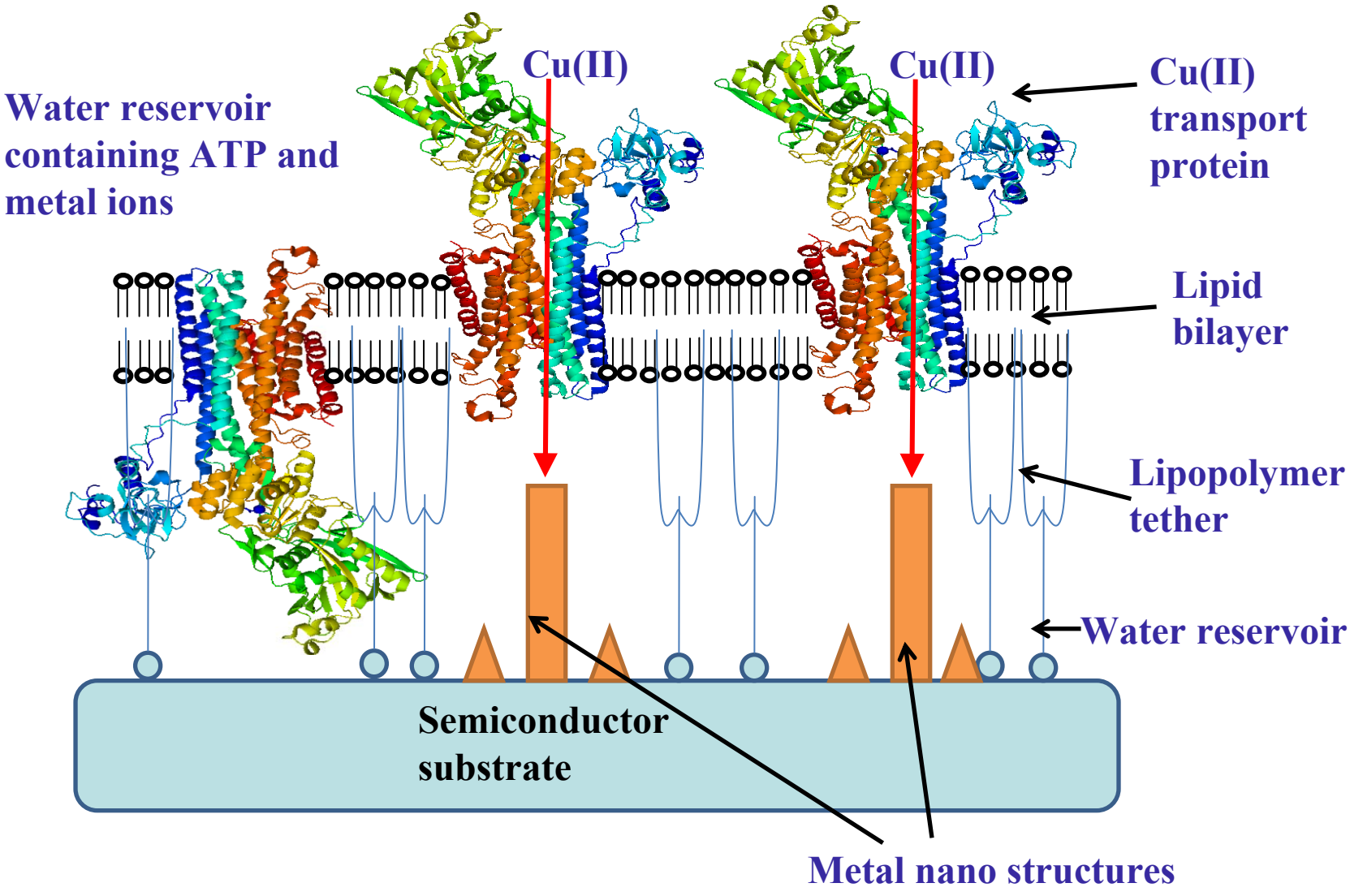

Characterization

Proteins

- **Explore fluorescence microscopy, fluorescence spectrometry and AFM as tools to characterize quantum-dot-tagged proteins**
- **Determine multi-color resolution of quantum-dot-tagged proteins in a lipid bilayer**

quantum dot – semiconductor nanocrystal

cadmium selenide, cadmium sulfide, cadmium telluride, indium arsenide

~2-10 nm in diameter

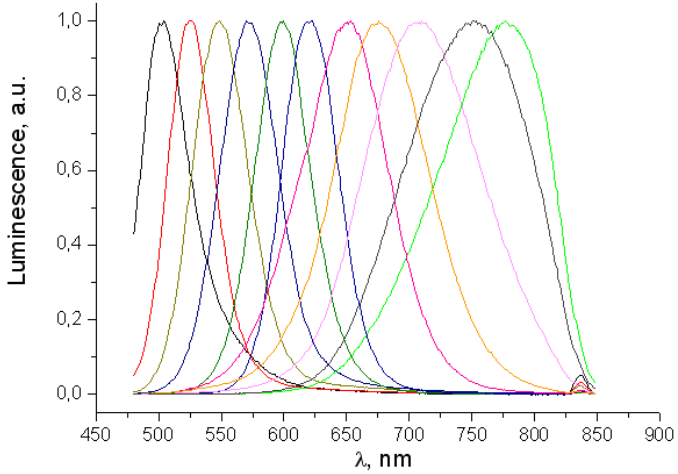

Fluorescence emission spectra of CdTe quantum dots of different sizes

Imaging with Quantum dots

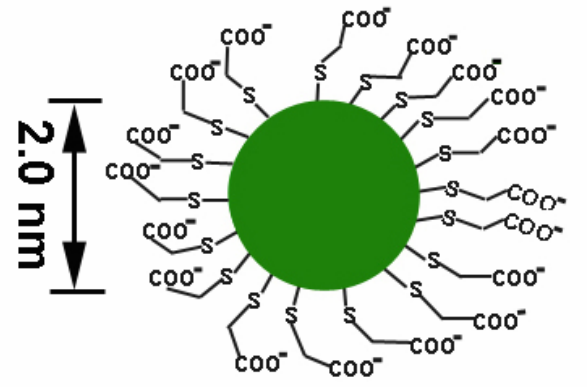

Single quantum dot terminated with COOH groups

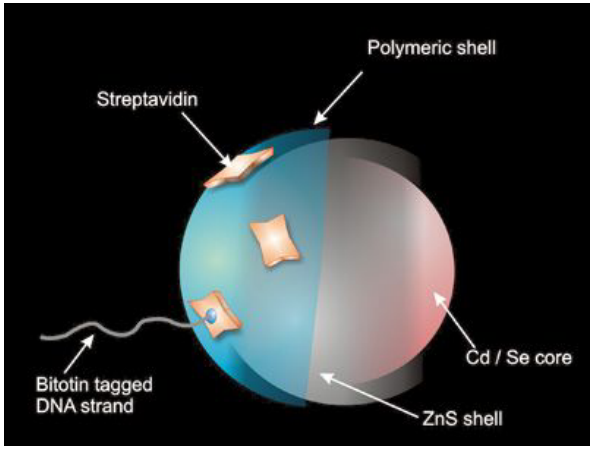

Functionalized quantum dot

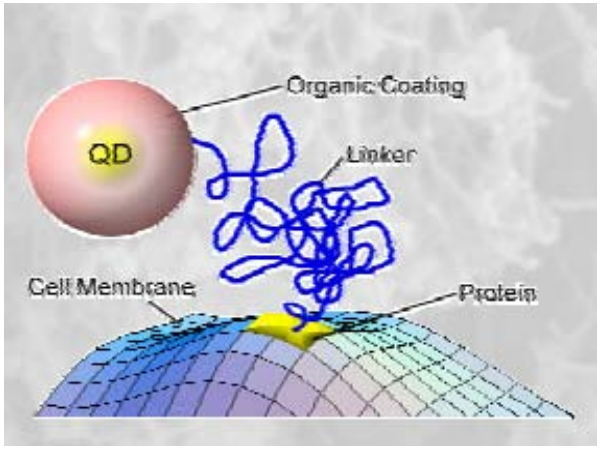

Quantum dot attached to protein with linker

Confocal Fluorescent Microscopy of Q-dots

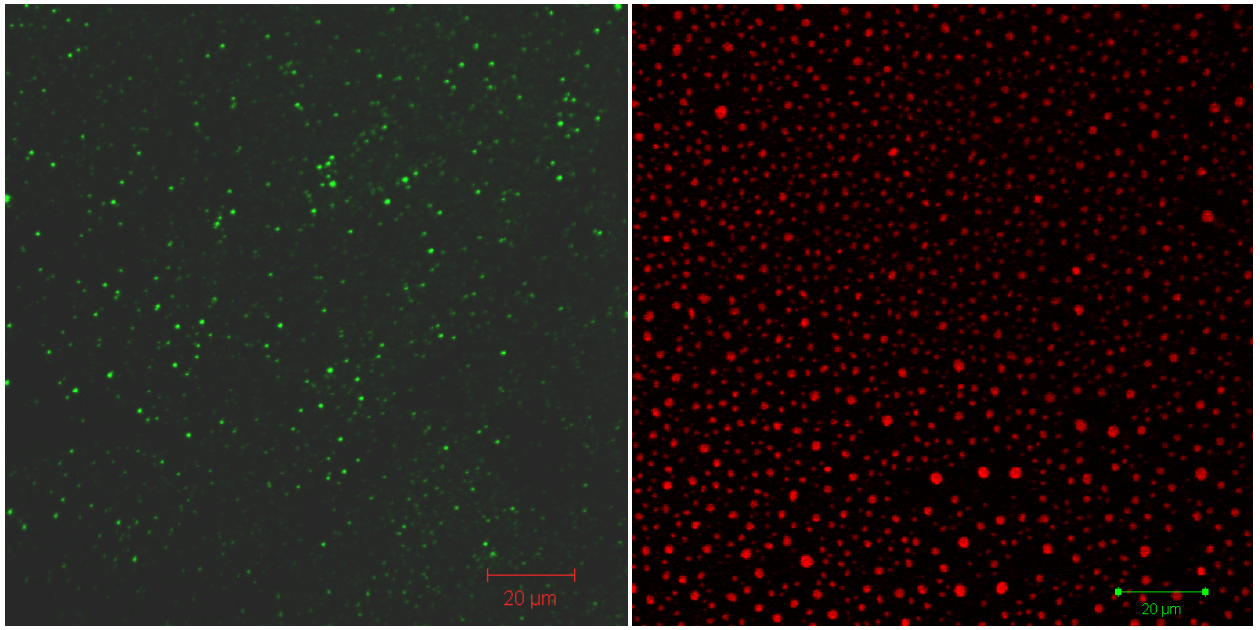

(Left) Green emission from CdSe quantum dots.
(Right) Red emission from CdTe quantum dots.

Imaging quantum dots and *A. fulgidus* CopB – Digital pulsed force mode image

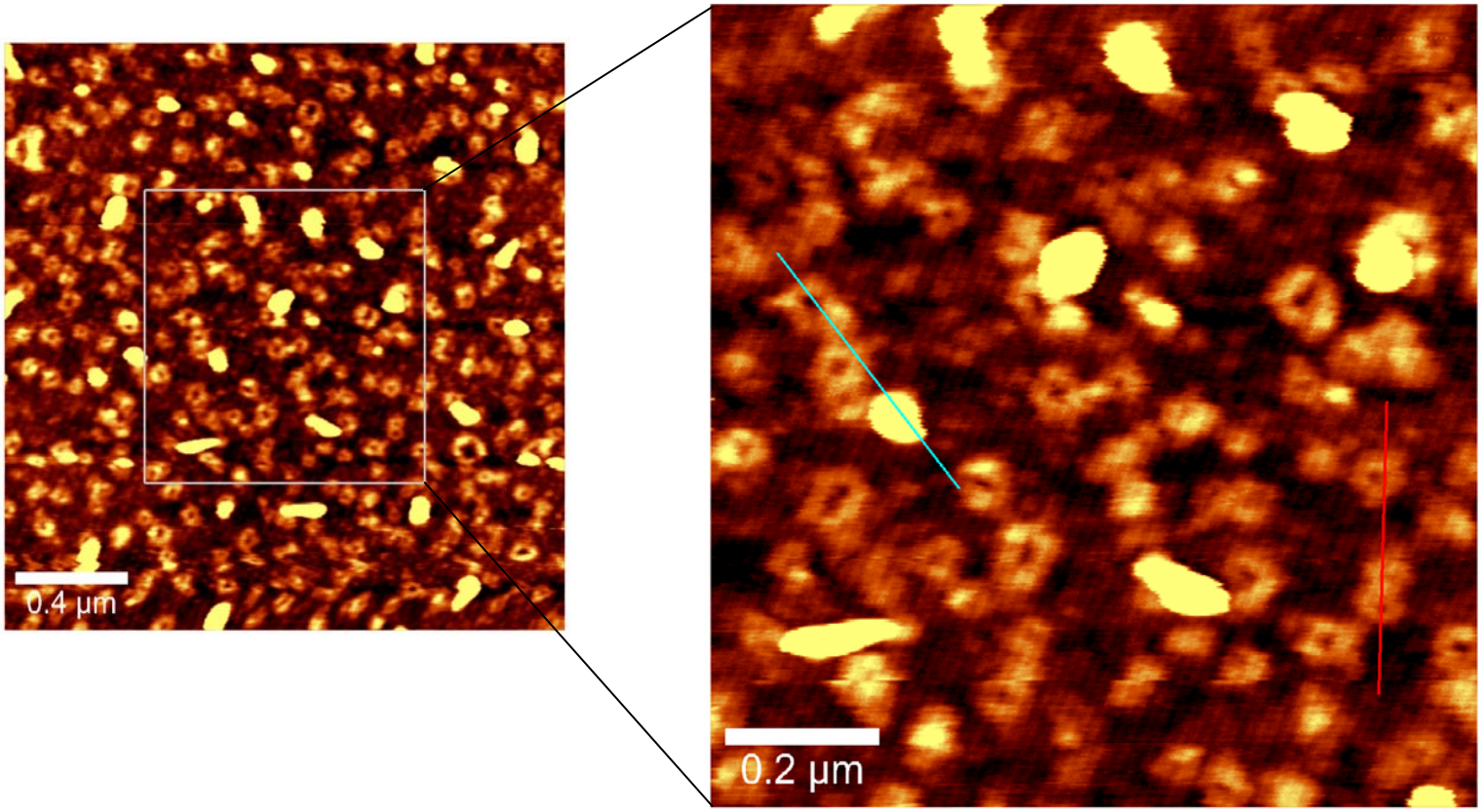

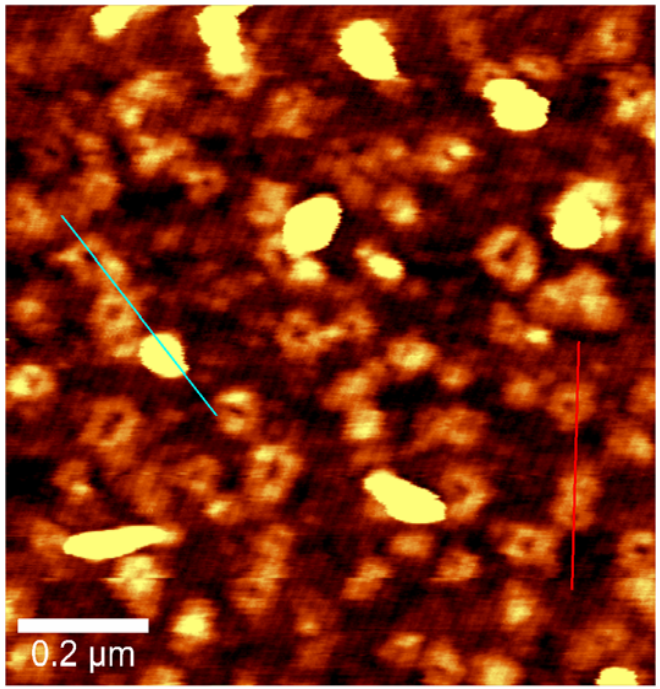

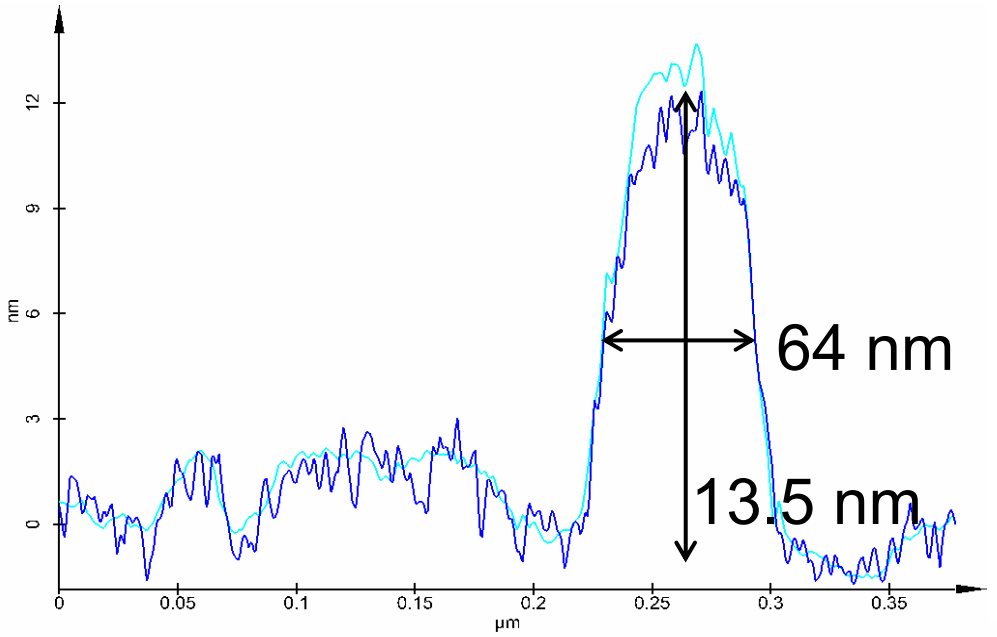

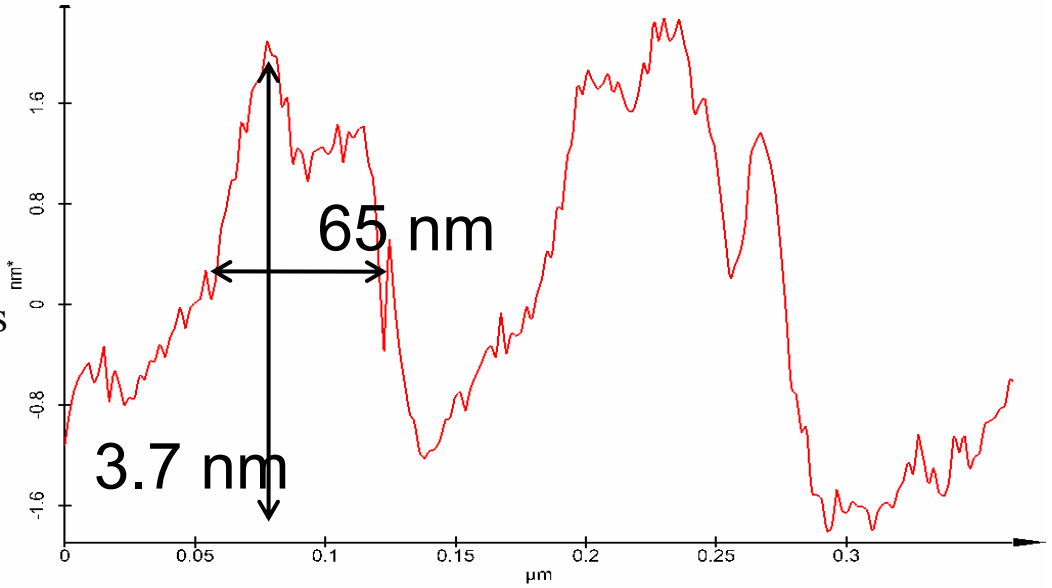

The red scan line traverses several proteins
The blue scan line crosses several proteins followed by quantum dots

Future Directions

- Optimize protein activity in artificial membranes
- Characterization of various potential substrates for lipid bilayer formation such as GaAs, Ge.
- Attachment of lipid bilayers to tethered semiconductor surfaces.
- Imaging the proteins in the lipid bilayer
- Imaging metal nano-structures

Acknowledgements

Science Foundation Arizona Strategic Research Group

SRC/SEMATECH Engineering Research Center for Environmentally Benign Semiconductor Manufacturing

ASM

SEZ

Technology and Research Infrastructure Fund (TRIF)